ESA Climate Change Initiative “Plus” (CCI+)

Product User Guide (PUG)

-

TROPOMI WFM-DOAS XCH_4

for the Essential Climate Variable (ECV)

Greenhouse Gases (GHG)

Written by:

GHG-CCI group at IUP

Lead author: O. Schneising, IUP, Univ. Bremen, Germany

Change log:

Version Nr.	Date	Status	Reason for change
Version 1	23 Oct 2019	Final	New document
Version 2	30 Oct 2020	Final	Update for CRDP#6
Version 2.1	08 Jan 2021	Final	Revision according to ESA's review
Version 3	12 Jul 2021	Final	Update for CRDP#7
Version 4	21 Aug 2023	Final	Update for CRDP#8
Version 5	31 May 2024	Final	Update for CRDP#9

31.05.2024

Product User Guide (PUG)

TROPOMI WFM-DOAS (TROPOMI/WFMD) XCH_4

Prepared by:

Oliver Schneising

Valid for:

TROPOMI/WFMD

Product	**Version**
Methane column-averaged dry air mole fraction (XCH_4)	v1.8

Contents

Spectrometer	SWIR	
Band ID	7	8
Spectral Range [nm]	2300 – 2343	2343 – 2389
Spectral Resolution FWHM [nm]	0.227	0.225
Spectral Sampling [nm]	0.094	
Spatial Sampling [km^2]	5.5×7	
Detector Binning Factor	1	

Table 1: Summary of the TROPOMI SWIR spectral bands and their key features (Ludewig, 2021).

1 Purpose of document

This document describes the TROPOMI WFM-DOAS (TROPOMI/WFMD) XCH_4 data product and illustrates how to use it.

2 Introduction

2.1 The TROPOMI instrument on Sentinel-5 Precursor

The TROPOspheric Monitoring Instrument (TROPOMI) is a spaceborne nadir viewing spectrometer with bands in the ultraviolet and visible (270-495 nm), the near infrared (675-775 nm) and the shortwave infrared (2305-2385 nm) (Veefkind et al., 2012). TROPOMI combines daily global coverage with a high spatial resolution in order to focus on the troposphere where concentrations of trace gas and aerosol species rapidly change. Light from different wavelength bands is measured by TROPOMI to generate various data products. Some of the species measured by TROPOMI include ozone, nitrogen dioxide, methane, and carbon monoxide.

Sentinel-5P was launched in October 2017 into a sun-synchronous orbit with an equator crossing time of 13:30. TROPOMI's observations of overtone absorptions in the shortwave infrared (SWIR) solar backscattered spectrum yield the vertical columns of CH_4 with high sensitivity down to the Earth's surface (Schneising et al., 2019). The instrument has a wide swath of 2600 km consisting of single measurements with a horizontal resolution of typically $5.5 \times 7\,km^2$ in the SWIR bands ($7 \times 7\,km^2$ before 6 August 2019). The characteristics of the TROPOMI SWIR bands are summarised in Table 1.

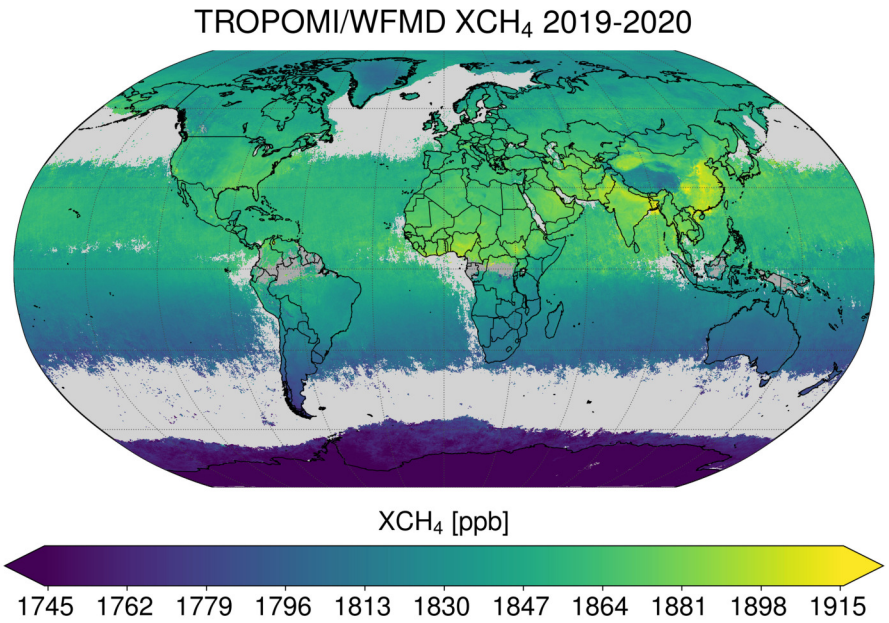

Figure 1: Biennial mean (2019-2020) of retrieved TROPOMI/WFMD v1.8 XCH_4.

2.2 The WFM-DOAS retrieval algorithm

The Weighting Function Modified Differential Optical Absorption Spectroscopy (WFM-DOAS) algorithm (Buchwitz et al., 2005a,b; Schneising et al., 2008, 2009, 2011, 2012; Heymann et al., 2012a,b; Schneising et al., 2013, 2014a,b, 2019, 2020a,b, 2023) is a least-squares method based on scaling (or shifting) pre-selected atmospheric vertical profiles. The column-averaged dry air mole fractions of methane (denoted XCH_4) are derived from the vertical column amounts of CH_4 by normalising with the dry air column, which is obtained from the European Centre for Medium-Range Weather Forecasts (ECMWF) ERA5 reanalysis. The corresponding vertical columns of CH_4 are retrieved from the measured sun-normalised radiance using spectral fitting windows in the SWIR spectral region (2311-2315.5 nm and 2320-2338 nm).

The global distribution of the retrieved mole fractions XCH_4 for the years 2019 and 2020 is shown in Figure 1. Clearly visible is the interhemispheric gradient with larger methane concentrations on the northern hemisphere, where the majority of sources is located, superimposed by enhancements over prominent source regions like anthropogenic emissions from fossil fuels and rice cultivation in China, India, and Southeast Asia. Other visible source regions include tropical wetlands as well as anthropogenic emissions in California or the Padan Plain in Italy.

From the validation with ground-based Fourier Transform Spectroscopy (FTS) measurements of the Total Carbon Column Observing Network (TCCON) (Wunch et al., 2011) at the TCCON sites listed in Table 2, realistic error estimates of the satellite data are provided and summarised in Table 3. For the sake of completeness, the error characteristics of XCO, which is simultaneously retrieved with XCH_4 and also included in the product, are also quoted.

Station	Latitude (°)	Longitude (°)	Altitude (km)	Reference GGG2020
Eureka	80.05	−86.42	0.61	Strong et al. (2022)
Ny-Ålesund	78.92	11.92	0.02	Buschmann et al. (2022)
Sodankylä	67.37	26.63	0.19	Kivi et al. (2022)
East Trout Lake	54.35	−104.99	0.50	Wunch et al. (2022)
Bremen	53.10	8.85	0.03	Notholt et al. (2022)
Harwell	51.57	−1.32	0.14	Weidmann et al. (2023)
Karlsruhe	49.10	8.44	0.11	Hase et al. (2022)
Paris	48.85	2.36	0.06	Té et al. (2022)
Orléans	47.97	2.11	0.13	Warneke et al. (2022)
Garmisch	47.48	11.06	0.75	Sussmann and Rettinger (2023)
Park Falls	45.94	−90.27	0.44	Wennberg et al. (2022b)
Rikubetsu	43.46	143.77	0.38	Morino et al. (2022a)
Xianghe	39.80	116.96	0.04	Zhou et al. (2022)
Lamont	36.60	−97.49	0.32	Wennberg et al. (2022c)
Tsukuba	36.05	140.12	0.03	Morino et al. (2022b)
Nicosia	35.14	33.38	0.19	Petri et al. (2022)
Edwards	34.96	−117.88	0.70	Iraci et al. (2022)
Caltech	34.14	−118.13	0.24	Wennberg et al. (2022a)
Saga	33.24	130.29	0.01	Shiomi et al. (2022)
Hefei	31.90	119.17	0.04	Liu et al. (2022)
Burgos	18.53	120.65	0.04	Morino et al. (2022c)
Darwin	−12.46	130.93	0.04	Deutscher et al. (2023b)
Réunion	−20.90	55.49	0.09	De Mazière et al. (2022)
Wollongong	−34.41	150.88	0.03	Deutscher et al. (2023a)
Lauder	−45.04	169.68	0.37	Sherlock et al. (2022)

Table 2: TCCON sites used in the validation ordered according to latitude from north to south.

	XCH_4 (ppb)	XCO (ppb)
Random Error	12.35	5.51
Systematic Error (spatio-temporal)	5.24	2.68

Table 3: Error characterisation of the WFM-DOAS data products (valid for TROPOMI/WFMD v1.8 XCH_4 and XCO). The figures of merit are derived for the TCCON release GGG2020.

3 Product description

The data product is based on TROPOMI Level 1b V01.00.00 (V02.00.00 since July 2021) files comprising spectra from the nominal operational mode, which started end of April 2018, and reprocessed spectra from the previous six-month commissioning phase.

3.1 Product content and format

The CH4-TROPOMI-WFMD data products are stored per day in seperate NetCDF-files (NetCDF-4 classic model). The product files contain the key product, i.e. the retrieved column-averaged dry air mole fractions XCH_4, as well as the column-averaged dry air mole fractions XCO and several other useful parameters (see Section 3.5 for details). Information relevant for the use of the data is also included in the data file, e.g. the averaging kernels.

3.2 Data usage

The column-averaged dry air mole fractions of methane are stored in the variable `xch4` in the NetCDF product files `ESACCI-GHG-L2-CH4-CO-TROPOMI-WFMD-YYYYMMDD-fv3.nc` (see Section 3.5).

If the data are to be compared with other data for which vertical profile information is available (e.g. comparison to models), the column averaging kernels should be applied to the model profiles using the formula

$$\mathrm{X}_{\mathrm{mod}} = \sum_l \Big(\mathrm{X}^l_{\mathrm{apr}} + A_l (\mathrm{X}^l_{\mathrm{mod}} - \mathrm{X}^l_{\mathrm{apr}}) \Big) w_l \qquad (1)$$

where l is the index of the vertical layer, A_l the averaging kernel (variables `xch4_averaging_kernel` and `xco_averaging_kernel` in NetCDF product files), $\mathrm{X}^l_{\mathrm{apr}}$ the a-priori mole fraction (variables `ch4_profile_apriori` and

`co_profile_apriori` in product files) and X^l_{mod} the simulated mole fraction of layer l. w_l is the layer dependent pressure weight (variable `pressure_weight` in product files).

3.3 Tools for reading the data

The data are stored in NetCDF format (NetCDF-4 classic model) which can be read with standard tools in the common programming languages (Python, IDL, Matlab, Fortran90, C++, etc).

3.4 Known limitations and issues

The file names `ESACCI-GHG-L2-CH4-CO-TROPOMI-WFMD-YYYYMMDD-fv3.nc` deviate slighty from the GHG-CCI file naming convention to take into a account that a comprehensive carbon monoxide mole fraction data set is also included in the product.

Data density (and potentially also data quality) is lower in the commissioning phase compared to the nominal operational mode, which started end of April 2018. Therefore, one may consider excluding data from the commissioning phase for sensitive applications.

3.5 Data file content

The structure of the Level2 product files `ESACCI-GHG-L2-CH4-CO-TROPOMI-WFMD-YYYYMMDD-fv3.nc` is summarised in the following:

```
netcdf ESACCI-GHG-L2-CH4-CO-TROPOMI-WFMD-20200701-fv3 {
dimensions:
    sounding_dim = 468201 ;
    level_dim = 21 ;
    layer_dim = 20 ;
    corners_dim = 4 ;
variables:
    double time(sounding_dim) ;
       time:standard_name = "time" ;
       time:long_name = "time" ;
       time:units = "seconds since 1970-01-01 00:00:00" ;
       time:calendar = "standard" ;
    float latitude(sounding_dim) ;
       latitude:standard_name = "latitude" ;
       latitude:long_name = "latitude" ;
       latitude:units = "degree_north" ;
       latitude:valid_range = -90.f, 90.f ;
       latitude:comment = "Center latitude of the measurement" ;
    float longitude(sounding_dim) ;
       longitude:standard_name = "longitude" ;
       longitude:long_name = "longitude" ;
       longitude:units = "degree_east" ;
       longitude:valid_range = -180.f, 180.f ;
       longitude:comment = "Center longitude of the measurement" ;
```

```
float solar_zenith_angle(sounding_dim) ;
   solar_zenith_angle:standard_name = "solar_zenith_angle" ;
   solar_zenith_angle:long_name = "solar_zenith_angle" ;
   solar_zenith_angle:units = "degree" ;
   solar_zenith_angle:comment = "Solar zenith angle is the the angle between the
            line of sight to the sun and the local vertical." ;
float sensor_zenith_angle(sounding_dim) ;
   sensor_zenith_angle:standard_name = "sensor_zenith_angle" ;
   sensor_zenith_angle:long_name = "sensor_zenith_angle" ;
   sensor_zenith_angle:units = "degree" ;
   sensor_zenith_angle:comment = "Sensor zenith angle is the the angle between the line
            of sight to the sensor and the local vertical." ;
float azimuth_difference(sounding_dim) ;
   azimuth_difference:long_name = "azimuth difference" ;
   azimuth_difference:units = "degree" ;
   azimuth_difference:comment = "Relative azimuth angle between sun and sensor direction." ;
float xch4(sounding_dim) ;
   xch4:standard_name = "dry_atmosphere_mole_fraction_of_methane" ;
   xch4:long_name = "column-averaged dry air mole fraction of atmospheric methane" ;
   xch4:units = "1e-9" ;
   xch4:comment = "Retrieved column-averaged dry air mole fraction of atmospheric
            methane (XCH4) in ppb" ;
float xch4_uncertainty(sounding_dim) ;
   xch4_uncertainty:long_name = "1-sigma uncertainty of the retrieved column-averaged
            dry air mole fraction of atmospheric methane" ;
   xch4_uncertainty:units = "1e-9" ;
   xch4_uncertainty:comment = "1-sigma uncertainty of the retrieved column-averaged
            dry air mole fraction of atmospheric methane (XCH4) in ppb" ;
int xch4_quality_flag(sounding_dim) ;
   xch4_quality_flag:long_name = "quality flag for the retrieved column-averaged
            dry air mole fraction of atmospheric methane" ;
   xch4_quality_flag:flag_values = 0, 1 ;
   xch4_quality_flag:flag_meanings = "good_quality potentially_bad_quality" ;
   xch4_quality_flag:comment = "0=good, 1=bad" ;
float xco(sounding_dim) ;
   xco:long_name = "column-averaged dry air mole fraction of atmospheric carbon monoxide" ;
   xco:units = "1e-9" ;
   xco:comment = "Retrieved column-averaged dry air mole fraction of atmospheric
            carbon monoxide (XCO) in ppb" ;
float xco_uncertainty(sounding_dim) ;
   xco_uncertainty:long_name = "1-sigma uncertainty of the retrieved column-averaged
            dry air mole fraction of atmospheric carbon monoxide" ;
   xco_uncertainty:units = "1e-9" ;
   xco_uncertainty:comment = "1-sigma uncertainty of the retrieved column-averaged
            dry air mole fraction of atmospheric carbon monoxide (XCO) in ppb" ;
int xco_quality_flag(sounding_dim) ;
   xco_quality_flag:long_name = "quality flag for the retrieved column-averaged
            dry air mole fraction of atmospheric carbon monoxide" ;
   xco_quality_flag:flag_values = 0, 1 ;
   xco_quality_flag:flag_meanings = "good_quality potentially_bad_quality" ;
   xco_quality_flag:comment = "0=good, 1=bad" ;
float pressure_levels(sounding_dim, level_dim) ;
   pressure_levels:long_name = "pressure levels" ;
   pressure_levels:units = "hPa" ;
   pressure_levels:comment = "Pressure levels define the boundaries of the
            averaging kernel and a priori profile layers.\n",
           "Levels are ordered from surface to top of atmosphere." ;
float pressure_weight(sounding_dim, layer_dim) ;
   pressure_weight:long_name = "pressure weight" ;
   pressure_weight:units = "1" ;
```

```
   pressure_weight:comment = "Layer dependent weights needed to apply the
            averaging kernels." ;
float ch4_profile_apriori(sounding_dim, layer_dim) ;
   ch4_profile_apriori:long_name = "a priori dry air mole fraction profile of
            atmospheric methane" ;
   ch4_profile_apriori:units = "1e-9" ;
   ch4_profile_apriori:comment = "A priori dry-air mole fraction profile of
            atmospheric methane in ppb.\n",
           "All values represent layer averages within the corresponding pressure levels.\n",
           "Profiles are ordered from surface to top of atmosphere." ;
float xch4_averaging_kernel(sounding_dim, layer_dim) ;
   xch4_averaging_kernel:long_name = "xch4 averaging kernel" ;
   xch4_averaging_kernel:units = "1" ;
   xch4_averaging_kernel:comment = "Represents the altitude sensitivity of the
            retrieval as a function of pressure.\n",
           "All values represent layer averages within the corresponding pressure levels.\n",
           "Profiles are ordered from surface to top of atmosphere." ;
float co_profile_apriori(sounding_dim, layer_dim) ;
   co_profile_apriori:long_name = "a priori dry air mole fraction profile of
            atmospheric carbon monoxide" ;
   co_profile_apriori:units = "1e-9" ;
   co_profile_apriori:comment = "A priori dry-air mole fraction profile of
            atmospheric carbon monoxide in ppb.\n",
           "All values represent layer averages within the corresponding pressure levels.\n",
           "Profiles are ordered from surface to top of atmosphere." ;
float xco_averaging_kernel(sounding_dim, layer_dim) ;
   xco_averaging_kernel:long_name = "xco averaging kernel" ;
   xco_averaging_kernel:units = "1" ;
   xco_averaging_kernel:comment = "Represents the altitude sensitivity of the
            retrieval as a function of pressure.\n",
           "All values represent layer averages within the corresponding pressure levels.\n",
           "Profiles are ordered from surface to top of atmosphere." ;
int orbit_number(sounding_dim) ;
   orbit_number:long_name = "orbit number" ;
   orbit_number:units = "1" ;
   orbit_number:comment = "Orbit number" ;
int scanline(sounding_dim) ;
   scanline:long_name = "along track dimension index" ;
   scanline:units = "1" ;
   scanline:comment = "This dimension variable defines the indices along track" ;
int ground_pixel(sounding_dim) ;
   ground_pixel:long_name = "across track dimension index" ;
   ground_pixel:units = "1" ;
   ground_pixel:comment = "This dimension variable defines the indices across track" ;
float latitude_corners(sounding_dim, corners_dim) ;
   latitude_corners:long_name = "latitude_corners" ;
   latitude_corners:units = "degree_north" ;
   latitude_corners:valid_range = -90.f, 90.f ;
   latitude_corners:comment = "Corner latitudes of the measurement" ;
float longitude_corners(sounding_dim, corners_dim) ;
   longitude_corners:long_name = "longitude_corners" ;
   longitude_corners:units = "degree_east" ;
   longitude_corners:valid_range = -180.f, 180.f ;
   longitude_corners:comment = "Corner longitudes of the measurement" ;
float altitude(sounding_dim) ;
   altitude:standard_name = "altitude" ;
   altitude:long_name = "altitude" ;
   altitude:units = "m" ;
   altitude:comment = "Average surface altitude" ;
float surface_roughness(sounding_dim) ;
```

```
      surface_roughness:long_name = "surface roughness" ;
      surface_roughness:units = "m" ;
      surface_roughness:comment = "Surface roughness" ;
   float apparent_albedo(sounding_dim) ;
      apparent_albedo:long_name = "apparent surface albedo" ;
      apparent_albedo:units = "1" ;
      apparent_albedo:comment = "Retrieved surface albedo at 2313nm" ;
   int land_fraction(sounding_dim) ;
      land_fraction:long_name = "land fraction" ;
      land_fraction:units = "1e-2" ;
      land_fraction:valid_range = 0, 100 ;
      land_fraction:comment = "Land fraction of the observed scene in percent" ;
   float cloud_parameter(sounding_dim) ;
      cloud_parameter:long_name = "cloud parameter from strong water vapour absorption" ;
      cloud_parameter:units = "1" ;
      cloud_parameter:comment = "Ratio of measured to cloud-free reference radiance
               for selected strong water vapour lines" ;
   float co_column(sounding_dim) ;
      co_column:long_name = "vertical column of carbon monoxide" ;
      co_column:units = "mol m-2" ;
      co_column:multiplication_factor_to_convert_to_molecules_percm2 = 6.022141e+19 ;
      co_column:comment = "Retrieved vertical column amount of carbon monoxide" ;
   float h2o_column(sounding_dim) ;
      h2o_column:long_name = "vertical column of water vapour" ;
      h2o_column:units = "g cm-2" ;
      h2o_column:comment = "Retrieved vertical column amount of water vapour" ;
   float h2o_column_uncertainty(sounding_dim) ;
      h2o_column_uncertainty:long_name = "1-sigma uncertainty of the retrieved vertical
               column of atmospheric water vapour" ;
      h2o_column_uncertainty:units = "g cm-2" ;
      h2o_column_uncertainty:comment = "1-sigma uncertainty of the retrieved vertical
               column of atmospheric water vapour" ;
   float satellite_altitude(sounding_dim) ;
      satellite_altitude:long_name = "satellite altitude" ;
      satellite_altitude:units = "m" ;
      satellite_altitude:valid_range = 700000.f, 900000.f ;
      satellite_altitude:comment = "Altitude of the spacecraft relative to the WGS84
               reference ellipsoid" ;
   float satellite_latitude(sounding_dim) ;
      satellite_latitude:long_name = "satellite latitude" ;
      satellite_latitude:units = "degrees_north" ;
      satellite_latitude:valid_range = -90.f, 90.f ;
      satellite_latitude:comment = "Latitude of the spacecraft sub-satellite point on
               the WGS84 reference ellipsoid" ;
   float satellite_longitude(sounding_dim) ;
      satellite_longitude:long_name = "satellite longitude" ;
      satellite_longitude:units = "degrees_east" ;
      satellite_longitude:valid_range = -180.f, 180.f ;
      satellite_longitude:comment = "Longitude of the spacecraft sub-satellite point on
               the WGS84 reference ellipsoid" ;

// global attributes:
   :title = "TROPOMI/WFMD XCH4 and XCO" ;
   :institution = "University of Bremen" ;
   :source = "TROPOMI L1B version 01.00.00" ;
   :history = "2022 - product generated with WFMD" ;
   :tracking_id = "e283f690-043f-480d-af8a-682ce9eeb060" ;
   :Conventions = "CF-1.6" ;
   :product_version = "v1.8" ;
   :summary = "Weighting Function Modified DOAS (WFMD) was adjusted to simultaneously
```

```
            retrieve column-averaged dry air mole fractions of atmospheric methane and
            carbon monoxide from the shortwave-infrared (SWIR) nadir spectra of the
            TROPOMI instrument onboard Sentinel-5 Precursor." ;
    :keywords = "satellite, Sentinel-5 Precursor, TROPOMI, atmosphere, methane, carbon monoxide" ;
    :id = "ESACCI-GHG-L2-CH4-CO-TROPOMI-WFMD-20200701-fv3.nc" ;
    :naming_authority = "iup.uni-bremen.de" ;
    :keywords_vocabulary = "NASA Global Change Master Directory (GCMD)" ;
    :cdm_data_type = "point" ;
    :comment = "These data were produced at the University of Bremen in the framework
            of the ESA GHG-CCI project" ;
    :date_created = "20220513T122550Z" ;
    :creator_name = "University of Bremen, IUP, Oliver Schneising" ;
    :creator_email = "schneising@iup.physik.uni-bremen.de" ;
    :project = "Climate Change Initiative - European Space Agency" ;
    :geospatial_lat_min = -90 ;
    :geospatial_lat_max = 90 ;
    :geospatial_lat_units = "degree_north" ;
    :geospatial_lon_min = -180 ;
    :geospatial_lon_max = 180 ;
    :geospatial_lon_units = "degree_east" ;
    :geospatial_vertical_min = 0 ;
    :geospatial_vertical_max = 100000 ;
    :time_coverage_start = "20200701T000000Z" ;
    :time_coverage_end = "20200701T235959Z" ;
    :time_coverage_duration = "P1D" ;
    :time_coverage_resolution = "P1D" ;
    :standard_name_vocabulary = "NetCDF Climate and Forecast (CF) Metadata Conventions
                Version 1.6" ;
    :license = "ESA CCI Data Policy: free and open access" ;
    :platform = "Sentinel-5 Precursor" ;
    :sensor = "TROPOMI" ;
    :spatial_resolution = "5.5km x 7km at nadir (typically)" ;
}
```

References

Buchwitz, M., de Beek, R., Burrows, J. P., Bovensmann, H., Warneke, T., Notholt, J., Meirink, J. F., Goede, A. P. H., Bergamaschi, P., Körner, S., Heimann, M., and Schulz, A.: Atmospheric methane and carbon dioxide from SCIAMACHY satellite data: initial comparison with chemistry and transport models, Atmos. Chem. Phys., 5, 941–962, https://doi.org/10.5194/acp-5-941-2005, 2005a.

Buchwitz, M., de Beek, R., Noël, S., Burrows, J. P., Bovensmann, H., Bremer, H., Bergamaschi, P., Körner, S., and Heimann, M.: Carbon monoxide, methane and carbon dioxide columns retrieved from SCIAMACHY by WFM-DOAS: year 2003 initial data set, Atmos. Chem. Phys., 5, 3313–3329, https://doi.org/10.5194/acp-5-3313-2005, 2005b.

Buschmann, M., Petri, C., Palm, M., Warneke, T., and Notholt, J.: TCCON data from Ny-Ålesund, Svalbard (NO), Release GGG2020.R0. TCCON data archive, hosted by CaltechDATA, California Institute of Technology, https://doi.org/10.14291/tccon.ggg2020.nyalesund01.R0, 2022.

De Mazière, M., Sha, M. K., Desmet, F., Hermans, C., Scolas, F., Kumps, N., Zhou, M., Metzger, J.-M., Duflot, V., and Cammas, J.-P.: TCCON data from Réunion Island (RE), Release GGG2020.R0. TCCON data archive, hosted by CaltechDATA, California Institute of Technology, https://doi.org/10.14291/tccon.ggg2020.reunion01.R0, 2022.

Deutscher, N. M., Griffith, D. W., Paton-Walsh, C., Jones, N. B., Velazco, V. A., Wilson, S. R., Macatangay, R. C., Kettlewell, G. C., Buchholz, R. R., Riggenbach, M. O., Bukosa, B., John, S. S., Walker, B. T., and Nawaz, H.: TCCON data from Wollongong (AU), Release GGG2020.R0. TCCON data archive, hosted by CaltechDATA, California Institute of Technology, https://doi.org/10.14291/tccon.ggg2020.wollongong01.R0, 2023a.

Deutscher, N. M., Griffith, D. W., Paton-Walsh, C., Velazco, V. A., Wennberg, P. O., Blavier, J.-F., Washenfelder, R. A., Yavin, Y., Keppel-Aleks, G., Toon, G. C., Jones, N. B., Kettlewell, G. C., Connor, B. J., Macatangay, R. C., Wunch, D., Roehl, C., and Bryant, G. W.: TCCON data from Darwin (AU), Release GGG2020.R0. TCCON data archive, hosted by CaltechDATA, California Institute of Technology, https://doi.org/10.14291/tccon.ggg2020.darwin01.R0, 2023b.

Hase, F., Herkommer, B., Groß, J., Blumenstock, T., Kiel, M., and Dohe, S.: TCCON data from Karlsruhe (DE), Release GGG2020.R0. TCCON data archive,

hosted by CaltechDATA, California Institute of Technology, https://doi.org/10.14291/tccon.ggg2020.karlsruhe01.R0, 2022.

Heymann, J., Schneising, O., Reuter, M., Buchwitz, M., Rozanov, V. V., Velazco, V. A., Bovensmann, H., and Burrows, J. P.: SCIAMACHY WFM-DOAS XCO_2: comparison with CarbonTracker XCO_2 focusing on aerosols and thin clouds, Atmos. Meas. Tech., 5, 1935–1952, https://doi.org/10.5194/amt-5-1935-2012, 2012a.

Heymann, J., Bovensmann, H., Buchwitz, M., Burrows, J. P., Deutscher, N. M., Notholt, J., Rettinger, M., Reuter, M., Schneising, O., Sussmann, R., and Warneke, T.: SCIAMACHY WFM-DOAS XCO_2: reduction of scattering related errors, Atmos. Meas. Tech., 5, 2375–2390, https://doi.org/10.5194/amt-5-2375-2012, 2012b.

Iraci, L. T., Podolske, J. R., Roehl, C., Wennberg, P. O., Blavier, J.-F., Allen, N., Wunch, D., and Osterman, G. B.: TCCON data from Edwards (US), Release GGG2020.R0. TCCON data archive, hosted by CaltechDATA, California Institute of Technology, https://doi.org/10.14291/tccon.ggg2020.edwards01.R0, 2022.

Kivi, R., Heikkinen, P., and Kyrö, E.: TCCON data from Sodankylä (FI), Release GGG2020.R0. TCCON data archive, hosted by CaltechDATA, California Institute of Technology, https://doi.org/10.14291/tccon.ggg2020.sodankyla01.R0, 2022.

Liu, C., Wang, W., Sun, Y., and Shan, C.: TCCON data from Hefei (PRC), Release GGG2020.R0, https://doi.org/10.14291/tccon.ggg2020.hefei01.R0. TCCONdataarchive,hostedbyCaltechDATA,CaliforniaInstituteofTechnology, 2022.

Ludewig, A.: S5P Mission Performance Centre Level 1b Readme, Reference: S5P-MPC-KNMI-PRF-L1B, Issue: 3.0.0, Product Version: V02.00.00, https://sentinel.esa.int/documents/247904/3541451/Sentinel-5P-Level-1b-Product-Readme-File, 2021.

Morino, I., Ohyama, H., Hori, A., and Ikegami, H.: TCCON data from Rikubetsu (JP), Release GGG2020.R0. TCCON data archive, hosted by CaltechDATA, California Institute of Technology, https://doi.org/10.14291/tccon.ggg2020.rikubetsu01.R0, 2022a.

Morino, I., Ohyama, H., Hori, A., and Ikegami, H.: TCCON data from Tsukuba (JP), 125HR, Release GGG2020.R0. TCCON data archive, hosted by Caltech-

DATA, California Institute of Technology, https://doi.org/10.14291/tccon.ggg2020.tsukuba02.R0, 2022b.

Morino, I., Velazco, V. A., Hori, A., Uchino, O., and Griffith, D. W. T.: TCCON data from Burgos, Ilocos Norte (PH), Release GGG2020.R0. TCCON data archive, hosted by CaltechDATA, California Institute of Technology, https://doi.org/10.14291/tccon.ggg2020.burgos01.R0, 2022c.

Notholt, J., Petri, C., Warneke, T., and Buschmann, M.: TCCON data from Bremen (DE), Release GGG2020.R0. TCCON data archive, hosted by CaltechDATA, California Institute of Technology, https://doi.org/10.14291/tccon.ggg2020.bremen01.R0, 2022.

Petri, C., Vrekoussis, M., Rousogenous, C., Warneke, T., Sciare, J., and Notholt, J.: TCCON data from Nicosia (CY), Release GGG2020.R0. TCCON data archive, hosted by CaltechDATA, California Institute of Technology, https://doi.org/10.14291/tccon.ggg2020.nicosia01.R0, 2022.

Schneising, O., Buchwitz, M., Burrows, J. P., Bovensmann, H., Reuter, M., Notholt, J., Macatangay, R., and Warneke, T.: Three years of greenhouse gas column-averaged dry air mole fractions retrieved from satellite - Part 1: Carbon dioxide, Atmos. Chem. Phys., 8, 3827–3853, https://doi.org/10.5194/acp-8-3827-2008, 2008.

Schneising, O., Buchwitz, M., Burrows, J. P., Bovensmann, H., Bergamaschi, P., and Peters, W.: Three years of greenhouse gas column-averaged dry air mole fractions retrieved from satellite - Part 2: Methane, Atmos. Chem. Phys., 9, 443–465, https://doi.org/10.5194/acp-9-443-2009, 2009.

Schneising, O., Buchwitz, M., Reuter, M., Heymann, J., Bovensmann, H., and Burrows, J. P.: Long-term analysis of carbon dioxide and methane column-averaged mole fractions retrieved from SCIAMACHY, Atmos. Chem. Phys., 11, 2863–2880, https://doi.org/10.5194/acp-11-2863-2011, 2011.

Schneising, O., Bergamaschi, P., Bovensmann, H., Buchwitz, M., Burrows, J. P., Deutscher, N. M., Griffith, D. W. T., Heymann, J., Macatangay, R., Messerschmidt, J., Notholt, J., Rettinger, M., Reuter, M., Sussmann, R., Toon, G. C., Velazco, V. A., Warneke, T., Wennberg, P. O., and Wunch, D.: Atmospheric greenhouse gases retrieved from SCIAMACHY: Comparison to ground-based FTS measurements and model results, Atmos. Chem. Phys., 12, 1527–1540, https://doi.org/10.5194/acp-12-1527-2012, 2012.

Schneising, O., Heymann, J., Buchwitz, M., Reuter, M., Bovensmann, H., and Burrows, J. P.: Anthropogenic carbon dioxide source areas observed from space: assessment of regional enhancements and trends, Atmos. Chem. Phys., 13, 2445–2454, https://doi.org/10.5194/acp-13-2445-2013, 2013.

Schneising, O., Reuter, M., Buchwitz, M., Heymann, J., Bovensmann, H., and Burrows, J. P.: Terrestrial carbon sink observed from space: variation of growth rates and seasonal cycle amplitudes in response to interannual surface temperature variability, Atmos. Chem. Phys., 14, 133–141, https://doi.org/10.5194/acp-14-133-2014, 2014a.

Schneising, O., Burrows, J. P., Dickerson, R. R., Buchwitz, M., Reuter, M., and Bovensmann, H.: Remote sensing of fugitive methane emissions from oil and gas production in North American tight geologic formations, Earth's Future, 2, 548–558, https://doi.org/10.1002/2014EF000265, 2014b.

Schneising, O., Buchwitz, M., Reuter, M., Bovensmann, H., Burrows, J. P., Borsdorff, T., Deutscher, N. M., Feist, D. G., Griffith, D. W. T., Hase, F., Hermans, C., Iraci, L. T., Kivi, R., Landgraf, J., Morino, I., Notholt, J., Petri, C., Pollard, D. F., Roche, S., Shiomi, K., Strong, K., Sussmann, R., Velazco, V. A., Warneke, T., and Wunch, D.: A scientific algorithm to simultaneously retrieve carbon monoxide and methane from TROPOMI onboard Sentinel-5 Precursor, Atmos. Meas. Tech., 12, 6771–6802, https://doi.org/10.5194/amt-12-6771-2019, 2019.

Schneising, O., Buchwitz, M., Reuter, M., Bovensmann, H., and Burrows, J. P.: Severe Californian wildfires in November 2018 observed from space: the carbon monoxide perspective, Atmos. Chem. Phys., 20, 3317–3332, https://doi.org/10.5194/acp-20-3317-2020, 2020a.

Schneising, O., Buchwitz, M., Reuter, M., Vanselow, S., Bovensmann, H., and Burrows, J. P.: Remote sensing of methane leakage from natural gas and petroleum systems revisited, Atmos. Chem. Phys., 20, 9169–9182, https://doi.org/10.5194/acp-20-9169-2020, 2020b.

Schneising, O., Buchwitz, M., Hachmeister, J., Vanselow, S., Reuter, M., Buschmann, M., Bovensmann, H., and Burrows, J. P.: Advances in retrieving XCH_4 and XCO from Sentinel-5 Precursor: improvements in the scientific TROPOMI/WFMD algorithm, Atmos. Meas. Tech., 16, 669–694, https://doi.org/10.5194/amt-16-669-2023, 2023.

Sherlock, V., Connor, B., Robinson, J., Shiona, H., Smale, D., and Pollard, D. F.: TCCON data from Lauder (NZ), 125HR, Release GGG2020.R0. TC-

CON data archive, hosted by CaltechDATA, California Institute of Technology, https://doi.org/10.14291/tccon.ggg2020.lauder02.R0, 2022.

Shiomi, K., Kawakami, S., Ohyama, H., Arai, K., Okumura, H., Ikegami, H., and Usami, M.: TCCON data from Saga (JP), Release GGG2020.R0. TCCON data archive, hosted by CaltechDATA, California Institute of Technology, https://doi.org/10.14291/tccon.ggg2020.saga01.R0, 2022.

Strong, K., Roche, S., Franklin, J. E., Mendonca, J., Lutsch, E., Weaver, D., Fogal, P. F., Drummond, J. R., Batchelor, R., Lindenmaier, R., and McGee, E.: TCCON data from Eureka (CA), Release GGG2020.R0. TCCON data archive, hosted by CaltechDATA, California Institute of Technology, https://doi.org/10.14291/tccon.ggg2020.eureka01.R0, 2022.

Sussmann, R. and Rettinger, M.: TCCON data from Garmisch (DE), Release GGG2020.R0. TCCON data archive, hosted by CaltechDATA, California Institute of Technology, https://doi.org/10.14291/tccon.ggg2020.garmisch01.R0, 2023.

Té, Y., Jeseck, P., and Janssen, C.: TCCON data from Paris (FR), Release GGG2020.R0. TCCON data archive, hosted by CaltechDATA, California Institute of Technology, https://doi.org/10.14291/tccon.ggg2020.paris01.R0, 2022.

Veefkind, J. P., Aben, I., McMullan, K., Förster, H., de Vries, J., Otter, G., Claas, J., Eskes, H. J., de Haan, J. F., Kleipool, Q., van Weele, M., Hasekamp, O., Hoogeveen, R., Landgraf, J., Snel, R., Tol, P., Ingmann, P., Voors, R., Kruizinga, B., Vink, R., Visser, H., and Levelt, P. F.: TROPOMI on the ESA Sentinel-5 Precursor: A GMES mission for global observations of the atmospheric composition for climate, air quality and ozone layer applications, Remote Sensing of Environment, 120, 70–83, https://doi.org/10.1016/j.rse.2011.09.027, 2012.

Warneke, T., Petri, C., Notholt, J., and Buschmann, M.: TCCON data from Orléans (FR), Release GGG2020.R0. TCCON data archive, hosted by CaltechDATA, California Institute of Technology, https://doi.org/10.14291/tccon.ggg2020.orleans01.R0, 2022.

Weidmann, D., Brownsword, R., and Doniki, S.: TCCON data from Harwell (UK), Release GGG2020.R0. TCCON data archive, hosted by CaltechDATA, California Institute of Technology, https://doi.org/10.14291/tccon.ggg2020.harwell01.R0, 2023.

Wennberg, P. O., Roehl, C., Wunch, D., Blavier, J.-F., Toon, G. C., Allen, N. T., Treffers, R., and Laughner, J.: TCCON data from Caltech (US), Release GGG2020.R0. TCCON data archive, hosted by CaltechDATA, California Institute of Technology, https://doi.org/10.14291/tccon.ggg2020.pasadena01.R0, 2022a.

Wennberg, P. O., Roehl, C. M., Wunch, D., Toon, G. C., Blavier, J.-F., Washenfelder, R., Keppel-Aleks, G., and Allen, N. T.: TCCON data from Park Falls (US), Release GGG2020.R1. TCCON data archive, hosted by CaltechDATA, California Institute of Technology, https://doi.org/10.14291/tccon.ggg2020.parkfalls01.R1, 2022b.

Wennberg, P. O., Wunch, D., Roehl, C. M., Blavier, J.-F., Toon, G. C., and Allen, N. T.: TCCON data from Lamont (US), Release GGG2020.R0. TCCON data archive, hosted by CaltechDATA, California Institute of Technology, https://doi.org/10.14291/tccon.ggg2020.lamont01.R0, 2022c.

Wunch, D., Toon, G. C., Blavier, J.-F. L., Washenfelder, R. A., Notholt, J., Connor, B. J., Griffith, D. W. T., Sherlock, V., and Wennberg, P. O.: The Total Carbon Column Observing Network, Phil. Trans. R. Soc. A, 369, 2087–2112, https://doi.org/10.1098/rsta.2010.0240, 2011.

Wunch, D., Mendonca, J., Colebatch, O., Allen, N. T., Blavier, J.-F., Kunz, K., Roche, S., Hedelius, J., Neufeld, G., Springett, S., Worthy, D., Kessler, R., and Strong, K.: TCCON data from East Trout Lake, SK (CA), Release GGG2020.R0. TCCON data archive, hosted by CaltechDATA, California Institute of Technology, https://doi.org/10.14291/tccon.ggg2020.easttroutlake01.R0, 2022.

Zhou, M., Wang, P., Kumps, N., Hermans, C., and Nan, W.: TCCON data from Xianghe, China, Release GGG2020.R0. TCCON data archive, hosted by CaltechDATA, California Institute of Technology, https://doi.org/10.14291/tccon.ggg2020.xianghe01.R0, 2022.